Applied Geochemistry 86 (2017) 70–83

Contents lists available at ScienceDirect

Applied Geochemistry

journal homepage: www.elsevier.com/locate/apgeochem

Comparing the $^{87}Sr/^{86}Sr$ of the bulk and exchangeable fractions in stream sediments: Implications for $^{87}Sr/^{86}Sr$ mapping in provenance studies

Yuka Jomori [a, b], Masayo Minami [a, *], Akiko Sakurai-Goto [c], Atsuyuki Ohta [d]

[a] Institute for Space-Earth Environmental Research, Nagoya University, Chikusa, Nagoya 464-8601, Japan
[b] Nishi Mikawa Citizens Affairs Office, Aichi Prefectural Government, Myodaiji-honmachi, Okazaki 444-8551, Japan
[c] School of Natural System, College of Science and Engineering, Kanazawa University, Kanazawa 920-1192, Japan
[d] Geological Survey of Japan, AIST, Tsukuba, Ibaraki 305-8568, Japan

ARTICLE INFO

Article history:
Received 15 May 2017
Received in revised form
12 August 2017
Accepted 4 September 2017
Available online 6 September 2017

Handling Editor: C. Reimann

Keywords:
$^{87}Sr/^{86}Sr$
Stream sediment
Stream water
Exchangeable fraction
Particle size
Geochemical map

ABSTRACT

We are preparing a nationwide distribution map of strontium isotope ratio ($^{87}Sr/^{86}Sr$) in Japan, using stream sediment to obtain basic $^{87}Sr/^{86}Sr$ data for the provenance analysis of food production and archaeological substances. To clarify the effect of particle size on $^{87}Sr/^{86}Sr$ in stream sediments, we analyzed stream sediment from the Shigenobu River system in Matsuyama, Ehime Prefecture, Japan, where a variety of silicate-dominated lithologies, that is, several bedrocks of andesitic, granitic, and siliciclastic sedimentary rocks, are distributed. This paper reports elemental concentrations and $^{87}Sr/^{86}Sr$ in stream sediments for six particle-size fractions (1000–500, 500–300, 300–180, 180–125, 125–75, and <75 μm). The results from stream sediments were compared with results from bedrock units and stream water over the catchment. The elemental concentrations in stream sediment tended to increase with decreasing particle size in all lithologies; however, Sr concentrations varied less than other elements across particle sizes. For most of the samples, $^{87}Sr/^{86}Sr$ varied by less than 0.001 among the six particle-size fractions, which was less than the variation among the different lithologies. Therefore, $^{87}Sr/^{86}Sr$ in the <180 μm particle-size fraction, which is normally used in Japanese nationwide geochemical mapping, should be a reliable proxy for bedrock $^{87}Sr/^{86}Sr$. The $^{87}Sr/^{86}Sr$ values in water samples from the Shigenobu River system were lower and less variable than $^{87}Sr/^{86}Sr$ in the stream sediments, and they did not faithfully correspond to the watershed geology. The inconsistency may reflect selective dissolution of Sr from plagioclase. Interestingly, $^{87}Sr/^{86}Sr$ values of the exchangeable fraction of stream sediment in the <180 μm fraction were strongly correlated with $^{87}Sr/^{86}Sr$ of stream water samples. Because $^{87}Sr/^{86}Sr$ in plant and animal bodies reflects that of their water sources, the exchangeable fraction of stream sediment may be a useful proxy for geochemical provenance in Japan instead of stream water.

1. Introduction

In addition to its utility in geology, the strontium isotopic ratio ($^{87}Sr/^{86}Sr$) is useful for identifying the origin of agricultural products and tracing the movements of ancient people (e.g., Kawasaki et al., 2002; Hodell et al., 2004; Bentley, 2006; Frei et al., 2009; Rummel et al., 2010; Thornton, 2011; Crowley et al., 2015). These applications are based on the fact that plants absorb water from the land where they grow, and human bones reflect the $^{87}Sr/^{86}Sr$ of the local water, plants, and animals that humans consume (e.g., Graustein, 1989; Voerkelius et al., 2010). Therefore, the regional distribution of $^{87}Sr/^{86}Sr$ on the surface is essential basic data for provenance studies of agricultural products and archaeological materials. All over the world, regional distribution maps of elemental concentrations have been created for mineral exploration and environmental assessment purposes using data from soils, stream sediments, surface water, and other sources (e.g., Caritat and Cooper, 2011; Fauth et al., 1985; Reimann et al., 1998; Salminen et al., 2005; Smith et al., 2014; Weaver et al., 1983; Webb et al., 1978; Zheng, 1994). Recently an attempt on making

* Corresponding author.
E-mail address: minami@isee.nagoya-u.ac.jp (M. Minami).

https://doi.org/10.1016/j.apgeochem.2017.09.004
0883-2927/

grobal scale $^{87}Sr/^{86}Sr$ maps is started for the provenance studies. For instance, Bataille and Bowen (2012) performed mapping $^{87}Sr/^{86}Sr$ variations in bedrock and water by investigating the links between bedrock geology and $^{87}Sr/^{86}Sr$ of stream/river water. Bataille et al. (2014) and Brennan et al. (2016) improved accuracy of predictions of $^{87}Sr/^{86}Sr$ using dendritic network models.

In Japan, the Geological Survey of Japan (GSJ), National Institute of Advanced Industrial Science and Technology (AIST) has compiled and published nationwide geochemical maps of 53 elements based on analyses of about 3000 samples of fine-grained (180 μm sieve) stream sediment (Imai et al., 2004). Asahara et al. (2006) compiled a regional Sr isotope ($^{87}Sr/^{86}Sr$) map using a similar <180 μm particle-size fraction, and they reported that the $^{87}Sr/^{86}Sr$ values of stream sediments changed systematically with the geology. The large scale mapping of $^{87}Sr/^{86}Sr$ in Japan is in preparation based on stream sediment samples (Jomori et al., 2013). Because stream sediment is a composite product of weathered and eroded soil and rocks in a catchment area that can provide information about the composition of local bedrock and mineral deposits (Howarth and Thornton, 1983), stream sediment is widely used for creating geochemical maps that are used for ore exploration, environmental assessments, and other purposes. However, it is still unclear to what extent the $^{87}Sr/^{86}Sr$ data from this fraction of stream sediment reflects the lithology in a drainage basin. Minami et al. (2017) thus investigated the effect of particle size on $^{87}Sr/^{86}Sr$ ratios in stream sediments collected from the granitic drainage basin by comparison of their values with those of the source rocks, and indicated that, in granite areas, the <180 μm fraction of the stream sediments can be used for $^{87}Sr/^{86}Sr$ mapping. Next, in this study, we investigate the effect of particle size on $^{87}Sr/^{86}Sr$ ratios in stream sediments collected from the drainage basin distributed by a variety of lithologies.

It is thought that $^{87}Sr/^{86}Sr$ of plant and animal tissues is directly related to $^{87}Sr/^{86}Sr$ in surface water, such as soil water and stream water as mentioned above. The relationships between $^{87}Sr/^{86}Sr$ of stream sediment, stream water, groundwater, and soil must be clarified before stream sediment can be considered a reliable proxy for use in geochemical provenance studies. To investigate this question, we collected samples of stream sediment and stream water from the Shigenobu River system in Matsuyama, Ehime Prefecture, Japan. The watershed of the Shigenobu River system includes a variety of lithologies of granitic rocks, siliceous sedimentary rocks, volcanic rocks, and metamorphic rocks, though the river system has short length (36 km) and small catchment.

We sieved the sediment samples into six size fractions (1000, 500, 300, 180, 125, and 75 μm) and measured elemental concentrations and $^{87}Sr/^{86}Sr$ in each fraction to clarify the effect of particle size of them. The distinct changes in lithology between the upper and lower reaches of the Shigenobu River system allowed us to elucidate the effect of lithology on elemental concentrations and $^{87}Sr/^{86}Sr$ in each particle-size fraction. We also analyzed stream water samples from the same locations as the sediment samples to investigate the relationship between $^{87}Sr/^{86}Sr$ values of stream water, stream sediment, and bedrock.

2. Sampling points and watershed geology

The Shigenobu River system drains a watershed with a wide variety of bedrock types (Fig. 1). Early to Late Cretaceous hornblende granodiorite (Ryoke granite) and metamorphic rocks (Ryoke metamorphic rocks) underlay the northern side of the watershed. The central part of the watershed is covered by Quaternary unconsolidated sediment and Late Cretaceous marine sedimentary rocks of the Izumi Group. The clastic rocks of the Izumi Group consist mainly of sandstone, shale, and tuff (Doi, 1964; Miyata et al., 1993). In the study area, the Izumi Group is predominantly conglomerate, sandstone, and mudstone (Miyazaki et al., 2016). Metamorphic rocks of the Sambagawa belt (mainly greenschist), Middle to Late Miocene andesitic volcanic rocks of the Ishizuchi Group, and early Eocene to early Oligocene sedimentary rocks of the Kuma Group underlie the southern part of the study area (Nagai, 1957; Suyari et al., 1991). The Kuma Group contains coarse clastic material that originated from the Izumi Group (Katto and Taira, 1979; Kihara, 1985). Hydrothermal alteration of the Kuma Group caused by the intrusion of Neogene volcanic rocks (mainly andesitic) has locally elevated the concentrations of heavy metals such as Cu, As, and Sb (Chiba et al., 2005; Sakakibara et al., 2005). Some Kieslager type Cu mines and Mn deposits are distributed nearby the Point 3 (Fig. 1), and associated with the Sambagawa metamorphic rocks (Suyari et al., 1991).

Matsuyama has a humid subtropical climate (Köppen climate classification: *Cfa*) with hot summers and cool winters. Precipitation is significant throughout the year, having the average annual precipitation of 1344 ± 254 mm/yr during 1890 and 2016 (Past precipitation data in Matsuyama provided by Japan Meteorological Agency). The Shigenobu River and the Ishide River have less than 10 m in width and less than 30 cm in depth at the upper streams and about 50 m in width for the main stream at Points 10, and create an alluvial fan of the Dougo Plain around Matsuyama City, covering an area of approximately 20 km from east to west and 17 km from north to south. There are many subterranean rivers flow beneath the Dougo Plain. Stream sediment and stream water were sampled at ten localities (Points 1–10) in the Shigenobu River and Ishide River systems, and two more samples of spring water were collected from Point 11 near Point 10, and Point 12 downstream from Point 9 (Fig. 1). The spring water is originated from the subterranean waters under the Dougo Plain.

We assumed that the most widely distributed bedrock unit in the watershed area is the dominant control of elemental abundances in stream sediments (Ohta et al., 2004). The proportion of each bedrock unit in the watershed area of the sampling points was calculated using Arc View GIS software (ESRI) (Table 1). Further details of our procedures are given in Ohta et al. (2004). The representative rock units cropping out over more than half of the watershed area are shown in Fig. 1: granitic rocks predominate around Points 1 and 2, sedimentary rocks of the Izumi and Kuma Groups around Points 3, 8, 9, and 10, and andesitic rocks of the Ishizuchi Group around Points 4, 5, 6, and 7. We also analyzed six stream sediment samples collected by the Japanese nationwide geochemical mapping project (Imai et al., 2004), shown in Fig. 1 along with their predominant bedrock units.

One conglomerate sample and two sandstone samples from the Izumi Group were analyzed for comparison with stream sediments. These were collected during geologic mapping in the Niihama region, northeast of the study area (Aoya et al., 2013).

3. Sample treatment and analytical method

Stream sediment samples were collected from the center flow part of the stream at the upper small streams of the Shigenobu River and the Ishide River, while collected from the bank part of the stream at their main streams. The collected samples were dried in air soon after bringing back to laboratory same as the AIST samples, and sieved into six particle-size fractions (1000–500, 500–300, 300–180, 180–125, 125–75, and <75 μm), though the AIST samples were sieved into <180 μm particle-fraction. The 1000–500 μm fraction accounted for about 40–60% of the total weight in most cases. The 500–300 μm fraction accounted for about 20–30%, the 300–180 μm fraction for 10–20%, the 180–125 μm fraction for 3–5%, the 125–75 μm fraction for 2–3%, and the <75 μm fraction

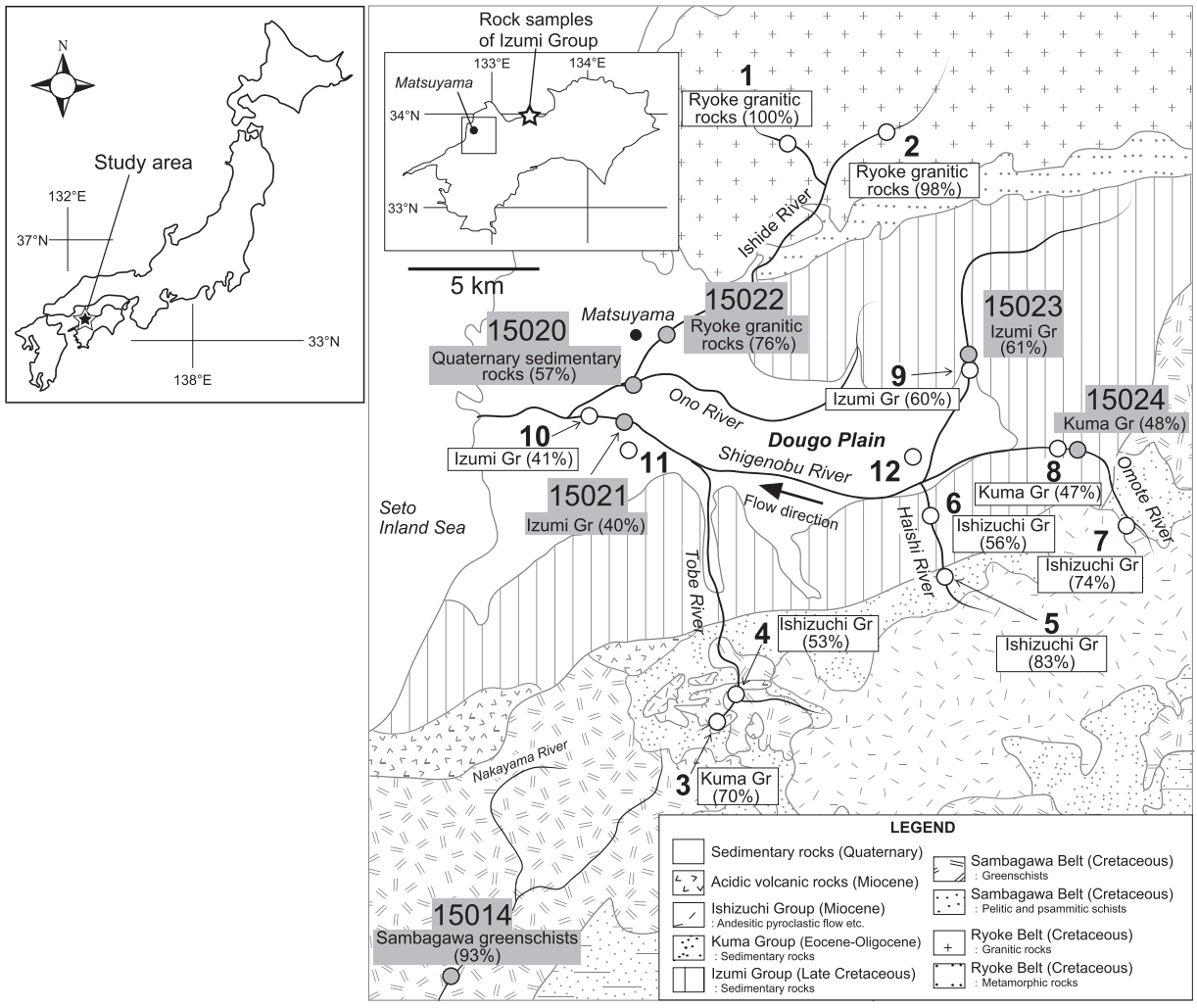

Fig. 1. Geologic map showing sampling points in the Shigenobu River system and the surrounding bedrock lithology. The predominant rock unit and its areal ratio are shown for each sampling point.

Table 1
Sampling point and proportion of bedrock geology in the watershed for stream sediments of the Shigenobu River system, Matsuyama, Ehime prefecture, Japan.

Sampling point	Representative bedrock	Proportion of rock unit (%)[a]						
		Gr	Rg	Qs	C-Ps		An	Sg
					Iz	Ku		
1	Granitic rock	100	–	–	–	–	–	–
2	Granitic rock	98	2	–	–	–	–	–
3	Sedimentary rock	–	–	–	–	70	30	0.5
4	Andesitic rock	–	–	–	–	37	53	10
5	Andesitic rock	–	–	–	–	17	83	–
6	Andesitic rock	–	–	–	–	44	56	–
7	Andesitic rock	–	–	–	–	26	74	–
8	Sedimentary rock	–	–	7	10	47	36	0.6
9	Sedimentary rock	10	30	–	60	–	–	–
10	Sedimentary rock	2	5	21	41	12	15	4
15014[b]	Greenschist	–	–	–	–	4	–	93
15020[b]	Sedimentary rock	1	–	57	42	–	–	–
15021[b]	Sedimentary rock	–	–	21	40	17	20	3
15022[b]	Granitic rock	76	13	3	9	–	–	–
15023[b]	Sedimentary rock	10	30	–	61	–	–	–
15024[b]	Sedimentary rock	–	–	6	9	48	37	0.6

[a] Gr, Ryoke granite; Rg, Ryoke gneiss; Qs, Quaternary sediment; C-Ps, Cretaceous to Paleogene sedimentary rocks including Izumi Group (Iz) and Kuma Group (Ku); An, andesitic volcanic rocks (dominantly Ishizuchi Group); Sg, Sambagawa greenschist.
[b] Samples were collected by AIST (Imai et al., 2004).

for 1–3%. All samples were milled with an agate mortar after sieving.

Major and trace elements were measured using an X-ray fluorescence (XRF) spectrometer (Shimadzu SXF-1800). After heating the powdered sediment for 5 h at 950 °C, 0.7 g samples were mixed with 6.0 g of $Li_2B_4O_7$ for major-element determinations, and 2.0 g samples were mixed with 3.0 g of $Li_2B_4O_7$ for trace-element determinations. The samples were then transferred to platinum crucibles and formed into glass beads using a high-frequency induction heating furnace at 1050 °C. XRF measurement was performed at 40 kV–70 mA for major elements and 40 kV–95 mA for trace elements.

The $^{87}Sr/^{86}Sr$ measurement procedure is described in detail by Jomori et al. (2013). For analysis of bulk fraction in stream sediments, the samples weighing 50–70 mg were heated at 900 °C for 2 h to remove organic matter and digested with $HF/HClO_4$. The product was evaporated to dryness and dissolved with 3 mL of 2.4 M HCl. The Sr in this solution was separated from the other elements using cation exchange resin (BioRad AG 50WX8, 200–400 mesh). The Sr isotopic ratios were measured by dynamic triple collector analysis using a magnetic sector-type thermal ionization mass spectrometer (VG Sector 54-30 at Nagoya University). The measured values were normalized for instrumental mass bias using a $^{86}Sr/^{88}Sr$ of 0.1194. The measured value of the repeat standard (NIST-SRM987) used during this study was 0.710243 ± 0.000016 (2σ, $n = 15$).

We also measured $^{87}Sr/^{86}Sr$ in the exchangeable (Ex) fraction of the sediment samples, which intends to extract elements in carbonates or those weakly adsorbed on materials. Approximately 200 mg of not thermally-dried sample was mixed with 10 mL of 1M ammonium acetate and left overnight in a PFA tube at room temperature. The supernatant solution was separated from the residue by centrifugation at 3500 rpm for 10 min. The solution, with a few drops of HNO_3 added, was evaporated to dryness and the residue was dissolved with 3 mL of 2.4 M HCl. The subsequent procedure was the same as the process for the sediment samples.

The water samples were filtered at the sampling points using a 0.45 μm cellulose acetate membrane filter. Aliquots of 300 mL were evaporated to dryness immediately after bringing back to laboratory, and the residue was dissolved with a few drops of HNO_3 and evaporated to dryness again. The residue was then dissolved with 3 mL of 2.4 M HCl, and divided into two aliquots. One was for the analysis of the Sr isotope ratio and the other for the analysis of Sr abundance. The latter was spiked with known amounts of ^{87}Rb (99.00%) and ^{84}Sr (80.53%) for the isotope dilution (ID) method. The procedures for Sr separation and isotopic measurement were similar to those for sediment samples. The Sr concentration in the water samples was measured with the ID method using a Finnigan MAT quadrupole mass spectrometer (THQ) at Nagoya University.

4. Results

The elemental concentrations of stream sediment by particle size and the $^{87}Sr/^{86}Sr$ determined for the bulk and Ex fractions in the sediment samples are summarized in Tables 2 and 3, respectively. Table 4 presents the results of chemical composition and $^{87}Sr/^{86}Sr$ of bedrock samples of Izumi Group. The Sr concentration and $^{87}Sr/^{86}Sr$ results for stream water and spring water are shown in Table 5.

4.1. Variation with particle size in elemental concentrations of stream sediment

Depending on the sediment size, shape, and density, detrital materials transported by rivers are segregated within the water column by hydrodynamic processes to concentrate fast-setting coarse and heavy minerals in bed loads while fine and light minerals preferentially in suspended load. Therefore, the mineral composition of stream sediment differs with particle size (e.g., Yagishita et al., 2000; Bouchez et al., 2010, 2011). For instance, quartz and K-feldspar are highly resistant to physical weathering (e.g., Goldich, 1938; White et al., 1996, 1997) and tend to be preserved in the coarser fractions. In our samples, the decrease in concentrations of SiO_2, Na_2O, K_2O, Rb, and Ba with decreasing particle size (Table 2 and Fig. 2) corresponds to the relative abundance of K-feldspar. Likewise, the increase in concentrations of Al_2O_3, P_2O_5, and CaO with decreasing particle size corresponds to the abundance of plagioclase, which is relatively susceptible to chemical weathering. The TiO_2, Fe_2O_3, and MgO concentrations, representing mafic and opaque minerals derived mainly from andesitic rocks (e.g., olivine, pyroxene, amphibole, magnetite, and ilmenite), were highest in the 300–125 μm fraction. Terashima et al. (2008) reported similar results from their geochemical study of stream sediment, finding, for instance, that coarse grains derived from granitic rocks were enriched in Na_2O and CaO and poor in K_2O and Ba.

Sediment from Points 1 and 2, representing areas of Ryoke granite, had very high concentrations of P_2O_5 and Zr in the fine fraction (<180 μm; Table 2 and Fig. 2), indicating that accessory minerals such as apatite and zircon were concentrated in fine particles. The X-ray diffraction patterns of the stream sediment at Point 1 showed a small Zircon peak in the <75 μm fraction, but not in the coarse fractions of 1000–500 and 300–180 μm. There was also an amphibole (hornblende) peak in the finest fraction. The sum of the evidence indicates that quartz and feldspar are distributed through all particle sizes whereas zircon, amphibole, and other heavy minerals are enriched in fine fractions.

In stream sediment from Point 3, the concentrations of Fe_2O_3, MnO, Co, Ni, Cu, and Zn increased in the <180 μm fractions; the concentration of Zn, in particular, increased from 1400 mg/kg in the coarsest fraction to 8400 mg/kg in the finest fraction. We attribute this extreme enrichment to mine waste, which represents hydrothermal deposits (pottery, Sb, and ferric sulfide ores) and Cu and Mn mines associated with the Sambagawa belt (Miyaji and Tsuzuki, 1988; Sakakibara et al., 2005).

Other than the extreme enrichment noted at Point 3, elemental concentrations faithfully reflected the parent lithology. For example, Points 4–7 within the Ishizuchi Group (mainly andesitic volcanic rocks) were relatively rich in TiO_2, Al_2O_3, Fe_2O_3, MgO, CaO, P_2O_5, and Sr and poor in Na_2O, K_2O, Rb, and Ba. As for Sr, the concentration systematically decreased from andesitic (Points 4–7) to granitic (Points 1 and 2) to sedimentary (Points 3, 8, 9, and 10) substrates. This result shows that Sr analyses based on sediment finer than 180 μm, the fraction generally used for Japanese geochemical mapping, are reliable.

4.2. Variation with particle size of $^{87}Sr/^{86}Sr$ in bulk and Ac soluble fractions of stream sediments

Fig. 3a shows that $^{87}Sr/^{86}Sr$ of stream sediment differed with the bedrock in the sediment catchment area. The area of the Izumi Group sedimentary rocks (Point 9) had the highest $^{87}Sr/^{86}Sr$ (0.7121–0.7126), the Ryoke granite (Points 1 and 2) had the second highest $^{87}Sr/^{86}Sr$ (0.7102–0.7108), and andesitic Ishizuchi Group (Points 4, 5, and 7) had the lowest $^{87}Sr/^{86}Sr$ (0.7074–0.7083). Points 6 and 8 had higher $^{87}Sr/^{86}Sr$ than the points upstream from them (Points 5 and 7, respectively) because their catchments included larger proportions of sediment from bedrock of the Kuma Group (Table 1). Point 10, on the lowest reach of the main stream of the Shigenobu River, had an intermediate $^{87}Sr/^{86}Sr$ value reflecting an

Table 2
Elemental concentrations of individual grain-size fractions in stream sediments in the Shigenobu River system, Ehime Prefecture, Japan.

Sampling point	1						2				3						4					
Grain size (μm)	1000 −500	500 −300	300 −180	180 −125	125 −75	<75	1000 −500	500 −300	180 −125	125 −75	1000 −500	500 −300	300 −180	180 −125	125 −75	<75	1000 −500	500 −300	300 −180	180 −125	125 −75	<75
Major elements (wt.%)																						
SiO_2	73.6	73.1	70.8	53.2	52.3	50.7	70.5	67.6	66.0	65.1	76.7	75.4	73.4	67.5	57.2	53.4	65.9	66.3	65.7	63.2	56.8	46.5
TiO_2	0.32	0.36	0.46	0.87	0.89	0.85	0.57	0.57	0.75	0.77	0.32	0.30	0.32	0.40	0.42	0.46	0.77	0.74	0.75	0.99	0.88	0.82
Al_2O_3	12.9	13.0	13.1	16.1	16.2	16.5	13.4	13.2	15.2	15.2	11.5	11.3	11.7	12.4	13.0	14.0	12.5	12.6	12.4	12.8	12.7	11.9
Fe_2O_3	2.43	2.73	3.49	6.67	6.85	6.86	4.41	4.68	4.44	4.74	3.54	3.56	3.93	6.14	9.16	11.0	6.91	6.54	6.34	6.59	6.48	6.01
MnO	0.05	0.06	0.08	0.18	0.18	0.18	0.07	0.08	0.11	0.11	0.09	0.08	0.10	0.17	0.35	0.46	0.14	0.12	0.11	0.11	0.13	0.12
MgO	0.60	0.69	0.90	1.75	1.77	1.81	1.01	1.13	1.34	1.41	0.38	0.39	0.49	0.60	0.63	0.72	2.25	2.16	1.92	1.97	1.88	1.99
CaO	1.51	1.60	1.89	2.66	2.69	2.90	1.70	1.84	2.28	2.56	0.42	0.41	0.50	0.64	0.80	0.86	2.50	2.33	2.15	2.51	2.59	2.30
Na_2O	2.61	2.55	2.55	2.12	2.04	2.10	2.79	2.77	3.41	3.52	1.58	2.06	1.50	1.62	1.17	0.95	1.88	1.92	1.85	1.71	1.57	1.45
K_2O	3.81	3.66	3.46	2.53	2.47	2.33	3.07	3.03	3.30	3.11	2.95	2.88	2.66	2.38	2.12	2.05	1.94	1.95	2.01	1.89	1.80	1.58
P_2O_5	0.06	0.07	0.08	0.43	0.46	0.50	0.08	0.09	0.08	0.09	0.04	0.04	0.04	0.06	0.10	0.14	0.10	0.09	0.09	0.13	0.21	0.24
L.O.I.	1.78	2.13	2.30	14.1	14.8	15.4	2.32	4.38	2.62	3.08	3.46	3.79	4.41	7.99	14.6	15.4	4.19	4.73	5.79	7.94	14.4	26.4
Total	99.6	99.9	99.1	101	101	100	99.9	99.3	99.5	99.8	101	100	99.0	99.7	99.3	99.5	99.0	99.4	99.0	99.9	99.4	99.3
Minor elements (mg/kg)																						
Ba	593	539	449	568	578	584	484	658	507	534	333	319	292	293	299	311	342	320	340	309	340	314
Co	6	7	9	31	31	31	16	18	16	19	21	20	22	46	74	81	38	36	34	37	36	33
Cr	11	13	26	33	33	37	36	12	28	55	54	54	57	63	76	89	108	106	105	117	135	103
Cu	n.d.	n.d.	n.d.	n.d.	n.d.	n.d.	n.d.	n.d.	n.d.	n.d.	26	27	33	78	197	265	n.d.	n.d.	n.d.	64	116	121
Ni	9	8	9	11	13	13	4	6	3	5	39	42	52	65	94	107	46	44	46	40	48	49
Pb	24	26	25	28	29	30	22	22	20	23	25	22	22	21	25	26	19	19	24	31	47	50
Rb	141	133	126	113	112	109	123	115	118	120	110	102	93	92	96	99	70	72	75	75	80	77
Sr	187	177	157	156	155	162	149	152	155	172	73	69	71	72	77	83	99	102	104	101	103	87
Th	6	8	9	24	29	30	11	48	56	35	9	10	9	11	8	13	5	5	6	6	4	5
V	21	21	27	69	78	79	37	39	45	53	49	49	51	56	61	63	122	112	107	123	120	115
Y	15	17	19	67	71	78	23	31	43	47	13	13	13	16	21	25	19	18	18	20	25	25
Zn	49	61	61	249	252	270	73	81	72	83	1425	1480	1841	3241	6372	8448	211	269	347	444	646	685
Zr	99	98	112	420	467	495	138	156	553	1461	100	101	97	114	112	112	111	109	105	114	139	124

Sampling point	5						6					7						8			
Grain size (μm)	1000−500	500−300	300−180	180−125	125−75	<75	1000−500	500−300	300−180	180−125	125−75	1000−500	500−300	300−180	180−125	125−75	<75	1000−500	500−300	300−180	180−125
Major elements (wt.%)																					
SiO_2	62.7	59.0	58.8	53.7	56.0	57.9	69.4	70.3	71.3	61.6	66.4	61.9	59.8	58.6	57.0	58.4	57.1	66.1	67.4	65.6	66.1
TiO_2	1.45	2.68	4.39	4.72	3.68	1.80	0.78	1.40	1.77	7.26	2.71	1.16	1.33	1.45	3.68	2.58	2.11	0.96	1.37	2.00	3.09
Al_2O_3	16.2	15.1	15.6	15.5	16.4	15.6	13.5	11.6	12.1	10.7	12.8	15.4	15.4	16.2	15.8	16.5	15.6	14.3	14.0	13.3	13.2
Fe_2O_3	5.25	7.41	9.47	8.81	7.83	5.75	4.27	4.59	5.01	10.3	5.70	5.24	5.74	5.95	7.44	6.88	6.41	4.32	5.21	6.27	6.75
MnO	0.09	0.13	0.16	0.16	0.14	0.13	0.07	0.08	0.09	0.17	0.10	0.09	0.11	0.11	0.14	0.12	0.11	0.07	0.09	0.11	0.11
MgO	1.78	2.88	3.72	3.18	2.73	1.97	1.20	1.45	1.69	2.23	1.67	2.07	2.25	2.38	2.67	2.40	2.09	1.41	1.81	2.40	1.96
CaO	3.58	3.66	3.91	4.29	4.32	3.56	2.12	1.88	1.92	1.91	2.09	2.75	2.94	3.35	3.68	3.67	3.16	2.68	2.58	2.47	2.22
Na_2O	2.62	2.29	2.04	2.74	2.20	2.18	2.09	1.84	1.80	1.56	1.89	2.39	2.26	2.23	2.32	2.34	2.17	2.44	2.30	2.11	2.00
K_2O	2.23	1.86	1.48	1.44	1.51	1.70	2.43	2.24	2.16	1.83	2.10	2.44	2.17	1.95	1.78	1.82	1.85	2.61	2.45	2.24	2.29
P_2O_5	0.19	0.15	0.13	0.14	0.17	0.24	0.13	0.08	0.08	0.09	0.11	0.17	0.14	0.12	0.10	0.11	0.17	0.15	0.12	0.10	0.10
L.O.I.	5.02	5.38	5.55	4.90	4.51	8.69	4.31	3.44	3.35	2.23	4.29	6.19	6.68	7.13	5.02	4.87	8.48	3.93	1.96	3.46	2.28
Total	101	101	105	99.6	99.4	99.5	100	98.9	101	99.8	99.8	99.8	98.7	99.4	99.6	99.6	99.3	99.0	99.3	100	100
Minor elements (mg/kg)																					
Ba	438	375	308	314	334	387	437	401	411	384	407	497	418	399	364	390	412	509	473	–	–
Co	21	36	47	43	37	26	16	20	22	53	26	23	26	26	37	31	29	16	21	–	–
Cr	48	90	116	117	124	95	49	70	74	103	125	52	59	61	80	73	70	42	60	–	–
Cu	12	10	7	7	9	15	10	8	3	7	7	n.d.	n.d.	n.d.	7	8	10	n.d.	n.d.	–	–

Ni	15	15	13	13	14	18	18	16	16	11	16	22	17	20	13	13	13	20	20	–	–
Pb	17	16	16	17	17	22	20	16	22	13	17	19	17	20	15	18	18	21	19	–	–
Rb	91	72	54	53	58	71	94	81	78	64	79	88	79	70	68	73	79	96	90	–	–
Sr	215	187	181	211	220	200	143	117	120	94	134	192	185	217	206	220	202	194	185	–	–
Th	7	4	n.d.	0.2	2	2	9	7	8	8	6	9	7	6	5	5	7	9	9	–	–
V	88	147	205	189	166	109	69	89	106	253	122	69	79	78	152	123	109	56	79	–	–
Y	19	17	13	13	16	23	18	17	15	16	17	20	16	17	16	18	28	21	20	–	–
Zn	65	85	113	101	94	93	72	71	76	101	83	83	76	94	96	94	97	75	91	–	–
Zr	166	148	129	136	221	418	153	132	127	188	275	175	157	135	156	190	615	157	143	–	–

Sampling point	9						10				
Grain size (μm)	1000–500	500–300	300–180	180–125	125–75	<75	1000–500	500–300	300–180	180–125	125–75
Major elements (wt.%)											
SiO_2	74.2	73.2	72.6	73.2	72.6	69.2	77.7	77.2	73.3	68.0	70.4
TiO_2	0.31	0.33	0.32	0.33	0.36	0.45	0.34	0.40	1.12	4.44	2.06
Al_2O_3	13.1	13.3	12.9	13.2	13.1	13.8	11.6	11.5	11.5	11.3	12.3
Fe_2O_3	2.86	3.06	2.93	2.82	2.79	3.32	2.41	2.75	3.86	6.29	4.55
MnO	0.05	0.05	0.05	0.05	0.06	0.09	0.04	0.05	0.06	0.12	0.08
MgO	0.71	0.75	0.71	0.73	0.72	0.89	0.58	0.81	1.14	1.31	1.02
CaO	0.79	0.80	0.75	0.71	0.71	0.82	0.96	1.03	1.19	1.26	1.27
Na_2O	2.57	2.48	2.51	2.57	2.44	2.30	2.42	2.34	2.25	2.23	2.39
K_2O	3.27	3.36	3.34	3.31	3.24	3.13	2.68	2.71	2.61	2.46	2.63
P_2O_5	0.06	0.05	0.05	0.05	0.05	0.09	0.07	0.07	0.06	0.07	0.09
L.O.I.	2.43	2.70	2.66	2.82	3.31	5.21	1.91	2.03	2.24	2.03	2.98
Total	100	100	98.8	99.7	99.3	99.3	101	101	99.3	99.6	99.8
Minor elements (mg/kg)											
Ba	528	550	566	526	608	595	539	541	541	472	500
Co	7	9	8	7	8	11	6	8	14	34	18
Cr	30	35	30	43	86	70	27	28	57	66	124
Cu	n.d.	6	3	3	4	11	n.d.	n.d.	n.d.	5	7
Ni	14	14	12	13	14	20	17	18	18	12	13
Pb	21	22	20	23	21	29	18	20	19	16	17
Rb	120	127	123	112	118	128	109	107	100	85	94
Sr	116	109	104	96	101	112	130	123	118	95	110
Th	10	12	11	13	11	9	9	9	10	12	8
V	42	43	42	36	44	53	32	38	61	132	81
Y	19	21	21	21	22	30	16	17	18	18	20
Zn	50	58	56	53	58	79	51	63	78	98	97
Zr	145	139	133	134	217	397	132	125	123	142	336

L.O.I., loss on ignition; n.d., not detected; –, not determined.

Table 3
$^{87}Sr/^{86}Sr$ results from stream sediments of the Shigenobu River system, Ehime Prefecture, Japan.[a]

Samping points	Fraction	Grain size (μm)					
		1000–500	500–300	300–180	180–125	125–75	<75
1	Bulk	0.710773 ± 14	0.710744 ± 14	0.710745 ± 20	0.710185 ± 16	0.710482 ± 14	0.710394 ± 14
	Ac leaching	0.709979 ± 13	0.709818 ± 14	0.709912 ± 13	0.709223 ± 13	0.709560 ± 16	0.709560 ± 16
2	Bulk	0.710501 ± 16	0.710843 ± 18	0.710602 ± 14	0.710494 ± 16	0.710216 ± 14	0.710146 ± 16
	Ac leaching	0.709974 ± 13	0.710054 ± 13	n.d.	0.709454 ± 13	0.709620 ± 13	0.709416 ± 11
3	Bulk	0.711844 ± 14	0.711739 ± 16	0.710970 ± 14	0.709772 ± 14	0.709136 ± 14	0.708870 ± 14
	Ac leaching	0.708392 ± 37	0.708252 ± 13	0.708258 ± 21	0.707972 ± 13	0.707985 ± 11	0.707996 ± 14
4	Bulk	0.707394 ± 16	0.707628 ± 18	0.707904 ± 14	0.707881 ± 14	0.707695 ± 16	0.708486 ± 14
	Ac leaching	0.707598 ± 11	0.707494 ± 13	n.d.	0.707640 ± 11	0.707716 ± 11	0.707611 ± 13
5	Bulk	0.707582 ± 14	0.707552 ± 14	0.707444 ± 13	0.707417 ± 16	0.707556 ± 16	0.707868 ± 16
	Ac leaching	0.707397 ± 13	0.707399 ± 11	0.707369 ± 13	0.707384 ± 14	0.707380 ± 13	0.707626 ± 13
6	Bulk	0.708781 ± 14	0.709092 ± 16	0.708970 ± 16	0.708871 ± 16	0.708735 ± 16	0.708816 ± 17
	Ac leaching	0.707705 ± 13	0.707728 ± 11	0.707703 ± 14	0.707421 ± 14	0.707629 ± 13	0.707646 ± 14
7	Bulk	0.707572 ± 18	0.707603 ± 14	0.707543 ± 14	0.707587 ± 16	0.707934 ± 14	0.708328 ± 14
	Ac leaching	0.707589 ± 14	0.707599 ± 13	0.707575 ± 13	0.707582 ± 13	0.707624 ± 11	0.707732 ± 11
8	Bulk	0.708100 ± 16	0.708343 ± 16	0.708473 ± 16	0.708825 ± 24	0.709382 ± 14 (<125 μm)	
	Ac leaching	0.708146 ± 11	0.708102 ± 13	0.708128 ± 11	0.708195 ± 13	0.708121 ± 13 (<125 μm)	
9	Bulk	0.712605 ± 16	0.712644 ± 26	0.712543 ± 17	0.712371 ± 16	0.712084 ± 14	0.712198 ± 14
	Ac leaching	0.709190 ± 11	0.708997 ± 14	0.708913 ± 13	0.708821 ± 13	0.708935 ± 11	0.708702 ± 11
10	Bulk	0.710690 ± 16	0.710703 ± 18	0.710346 ± 16	0.710149 ± 16	0.710321 ± 16	0.710490 ± 16
	Ac leaching	0.709012 ± 11	0.708701 ± 11	0.708625 ± 11	0.708552 ± 13	0.708668 ± 13	0.708526 ± 11

AIST samples	Fraction	
15014	Bulk	0.704859 ± 17
	Ac leaching	0.707764 ± 13
15020	Bulk	0.711780 ± 14
	Ac leaching	0.707605 ± 11
15021	Bulk	0.710666 ± 13
	Ac leaching	0.709030 ± 13
15022	Bulk	0.708257 ± 14
	Ac leaching	0.708009 ± 11
15023	Bulk	0.712524 ± 14
	Ac leaching	0.709024 ± 13
15024	Bulk	0.709201 ± 14
	Ac leaching	0.708258 ± 14

[a] Errors in the final digits are 2σ level.

average of all the stream sediments in the study area (0.7101–0.7107).

The variation in $^{87}Sr/^{86}Sr$ with particle size appeared to differ in accordance with the representative geology of the catchment area. The $^{87}Sr/^{86}Sr$ values for stream sediment from areas of both granitic and sedimentary rocks (Points 1, 2, 9, and 10) decreased with decreasing particle size, and $^{87}Sr/^{86}Sr$ of stream sediment in the area of andesitic volcanic rocks (Points 4–7) increased with decreasing particle size. The greatest such fluctuation in $^{87}Sr/^{86}Sr$ with particle size was in the stream sediment from Point 3. This suggests a possibility, discussed further below, that the origin and mixing ratio of the clastics differ with particle size.

The $^{87}Sr/^{86}Sr$ variation with grain size in the Ex fraction was much smaller than in the bulk fraction: $^{87}Sr/^{86}Sr$ values in the Ex fraction from fine grains were systematically but slightly (0.0003) lower than those from coarse grains (Fig. 3b). The $^{87}Sr/^{86}Sr$ values in the Ex fraction decreased systematically from granitic (Points 1 and 2) to sedimentary (Points 3, 8, 9, and 10) to andesitic (Points 4–7) substrates.

4.3. Comparison of $^{87}Sr/^{86}Sr$ in stream water and stream sediment

Stream water samples had consistently lower $^{87}Sr/^{86}Sr$ than the bulk fraction of stream sediment at all points, but had almost identical $^{87}Sr/^{86}Sr$ to that in the Ex fractions (Fig. 4). The differences in $^{87}Sr/^{86}Sr$ between the bulk and Ex fractions were systematically larger from andesitic rocks (Points 5 and 7) to granitic rocks (Points 1 and 2) to sedimentary rocks (Points 3, 8, 9, and 10). Points 4 and 6, in areas of andesitic volcanic rocks, had larger differences than Points 5 and 7, which we attribute to the contribution of Sr originating from the sedimentary Kuma Group at Points 4 and 6 (Table 1). The Sr concentrations and $^{87}Sr/^{86}Sr$ of the spring water samples from Points 11 and 12 nearly matched those of stream water samples from nearby Points 10 and 9, respectively (Table 3). This is because these spring waters originate from subterranean rivers, which are derived from the Shigenobu River water, flowing beneath the surface of the Dougo Plain.

5. Discussion

5.1. Controlling factors of variation in elemental concentrations and $^{87}Sr/^{86}Sr$

The variations of elemental concentrations and $^{87}Sr/^{86}Sr$ over different geological substrates (granitic, andesitic, and sedimentary rocks) appear to be greater than the variation among particle-size fractions (Figs. 2 and 3). To evaluate this difference, we applied two-way analysis of variance (ANOVA) to infer whether the stronger controlling factor is geology or particle size (Miller and Miller, 2010). Our procedure for application of ANOVA to geochemical data followed those described by Ohta et al. (2010).

Geochemical data usually follow either a normal distribution or a lognormal distribution. The Shapiro-Wilk test was applied to test for the normality to each data set using a confidence level of probability (p) = 0.01 (Shapiro and Wilk, 1965). The results show that the data for 8 elements such as SiO_2 and Rb and $^{87}Sr/^{86}Sr$ follow a normal distribution and the log-transformed data for MnO, P_2O_5, Co, Ni, Sr, and V follow a normal distribution (Table 6). The

Table 4
Elemental concentrations and $^{87}Sr/^{86}Sr$ in rock samples of the Izumi Group, Ehime Prefecture, Japan.

	Sandstone 1	Sandstone 2	Conglomerate
Major elements (wt.%)			
SiO_2	78.6	79.0	76.3
TiO_2	0.17	0.20	0.10
Al_2O_3	12.2	12.2	13.9
Fe_2O_3	0.72	0.49	0.89
MnO	0.01	0.01	0.02
MgO	0.10	0.09	0.001
CaO	0.29	0.17	0.13
Na_2O	2.66	3.14	7.31
K_2O	3.62	3.35	0.18
P_2O_5	0.03	0.01	0.01
L.O.I.	1.87	0.52	1.03
Total	100	99.1	99.9
Minor elements (mg/kg)			
Ba	712	800	734
Co	n.d.	20	5
Cr	123	157	303
Cu	n.d.	n.d.	n.d.
Ni	24	26	39
Pb	22	12	18
Rb	143	134	122
Sr	90	118	121
Th	15	11	10
V	11	16	32
Y	19	14	22
Zn	27	8	29
Zr	157	203	150
$^{87}Sr/^{86}Sr$	0.713498 ± 11	0.712273 ± 13	0.712083 ± 13

data for the remaining elements (TiO_2, Al_2O_3, Ba, Pb, Th, Y, Zn, and Zr) followed neither a normal nor a lognormal distribution. In such cases, Ohta et al. (2005) proposed that the data distribution with skewness closer to zero (i.e., closer to normal) be used for ANOVA. As a result, the concentrations of the remaining elements were log-transformed.

Table 6 also presents the result of ANOVA. When the p is less than 0.01, we concluded that the factor made a statistically significant difference for the chemical composition or isotopic ratio. If two or three factors had $p < 0.01$, the factor having the largest product of degree of freedom and the variance ratio (F) value was considered the most dominant. Our ANOVA results show that the effect of the geologic factor is significant for all data except MnO, Pb, and Zn concentrations, the effect of grain size is significant for concentrations of seven elements, especially for those of MnO and Zr, but not significant for $^{87}Sr/^{86}Sr$, and the effect of both factors is not significant for Pb and Zn concentrations. The results suggest that elemental concentrations and $^{87}Sr/^{86}Sr$ ratios in stream sediments are dominantly controlled by the bedrock lithology around the sampling point, whereas MnO and Zr concentrations are influenced predominantly by the particle size and neither factor is predominant for Pb and Zn. The most important finding from this analysis is that Rb and Sr concentrations and $^{87}Sr/^{86}Sr$ in stream sediment are primarily controlled by substrate lithology. The same result was obtained for $^{87}Sr/^{86}Sr$ ratio in the Ex fraction.

5.2. Geochemical variations with particle size at Point 3

The variation with particle size in concentrations of Fe_2O_3, Co, Ni, Cu, Zn, and Pb and in $^{87}Sr/^{86}Sr$ was especially great in the sample from Point 3 (Figs. 2 and 3). Of the watershed area of Point 3, 70% consists of sedimentary rocks of the Kuma Group and 21% consists of andesitic volcanic rocks that are concentrated near Point 3 (Fig. 1 and Table 1). The range of $^{87}Sr/^{86}Sr$ in the coarse size fraction at Point 3 was 0.7110–7118, which was higher than values in the coarse fraction from Points 1 and 2, originating from Ryoke granite, and lower than those of Point 9, originating from the Izumi Group. Therefore, the coarse fraction appears to represent the Kuma Group sedimentary rocks. The $^{87}Sr/^{86}Sr$ ratios decreased steeply with decreasing grain size (Fig. 3), and in the finest fraction they matched those of Point 6, where the sediment originated from the andesitic volcanic rocks of the Ishizuchi Group. However, the Sr concentrations in the Point 3 sample scarcely changed with particle size whereas in the fine fraction the concentrations of SiO_2, Na_2O, K_2O, Rb, and Ba decreased and concentrations of Al_2O_3, MgO, CaO, and P_2O_5 increased (Table 2 and Fig. 2). These results suggest that plagioclase, K-feldspar, and orthopyroxene from the Kuma Group and andesitic volcanic rocks were altered by hydrothermal activity to clay minerals (illite, kaolinite, and chlorite), which were retained in the fine fraction.

The proportions of amphibole and pyroxene, which are the main minerals in andesite, were larger in the finer particles. Because hydrothermal alteration has weakened the andesite, and because the constituent mineral grains in andesite are generally smaller than 0.1 mm, mafic minerals from altered andesite could be disproportionately present in the finer particles at Point 3. The decrease in K_2O concentration with decreasing particle size may reflect the smaller proportion of K-feldspar, which is relatively resistant to weathering, in the finer size fraction.

The large variation in $^{87}Sr/^{86}Sr$ with particle size in the Point 3 sediment can be explained by the fact that Point 3 is in the upper reach of its tributary, where weathering is incomplete and clastics of different sources are mixed. Many streams share this setting in Japan, where the undulating topography produces abundant slopes with steep gradients. Sediments in the upper reaches of streams with a variety of lithologies in their catchment areas may be likely to feature chemical compositions and isotopic ratios that vary strongly with grain size.

Table 5
$^{87}Sr/^{86}Sr$ of stream water and spring water of the Shigenobu River system, Ehime Prefecture, Japan.

Sampling Point	Sample type	$^{87}Sr/^{86}Sr$	Sr concentration (mg/kg)
1	Stream water	0.709890 ± 16	0.118
2	Stream water	0.709466 ± 17	0.0374
3	Stream water	0.708047 ± 13	0.249
4	Stream water	0.707337 ± 16	0.0978
5	Stream water	0.707316 ± 16	0.0384
6	Stream water	0.707505 ± 14	0.0563
7	Stream water	0.707516 ± 14	0.0252
8	Stream water	0.708074 ± 16	0.0688
9	Stream water	0.708619 ± 14	0.179
10	Stream water	0.708484 ± 14	0.158
11	Spring water	0.708342 ± 14	0.137
12	Spring water	0.708659 ± 16	0.177

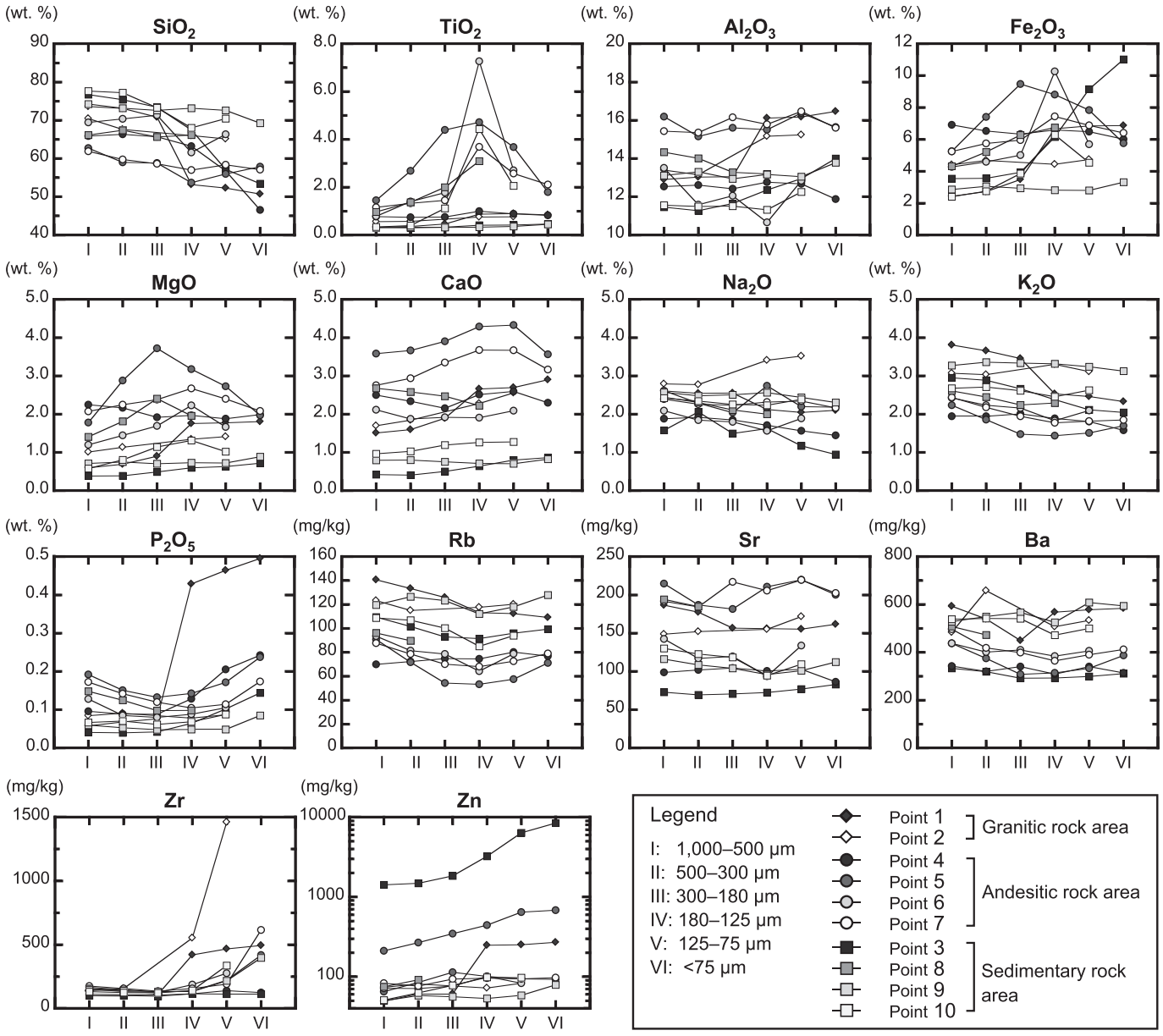

Fig. 2. Major- and trace-element concentrations of stream sediments according to particle size.

5.3. Estimation of Rb and Sr concentrations and $^{87}Sr/^{86}Sr$ of parent lithologies by regression analysis

Here we test if we could predict the Rb/Sr and $^{87}Sr/^{86}Sr$ of bedrock samples based on the stream sediment fraction. We sought to model how the Rb and Sr concentrations and $^{87}Sr/^{86}Sr$ in stream sediments vary with the watershed geology by using a multiple linear regression expressed as follows:

$$X = \sum_i f_i A_i X_i / A_T$$

where X is the Rb or Sr concentration or $^{87}Sr/^{86}Sr$ in stream sediment at a sampling point, X_i is the portion of X derived from an individual lithology, f_i is a factor of sediment production (resistance to denudation of a lithology, slope gradient, vegetation coverage, river morphology, and so on), A_i is the exposed area of each lithology, and A_T is the total area of the drainage basin. In this study, we fixed f_i at unity so that the elemental concentrations and $^{87}Sr/^{86}Sr$ in stream sediments are simply a function of the exposed area of each lithology (A_i/A_T).

We simplified the lithologic variety in the study area from seven to three groups. For calculation of $^{87}Sr/^{86}Sr$, we combined Ryoke gneiss (Rg in Table 1) with Ryoke granite (Gr), because Ryoke gneiss never exceeds 30% of a watershed. For calculating Rb and Sr concentrations, we combined Izumi Group, Kuma Group, and Quaternary sediments (Iz, Ku, and Qs in Table 1) as “Sedimentary rocks” (Sed) and combined the andesite and Sambagawa rocks (An and Sg) into “An and Sg” because the partial regression coefficients for the individual units were not significant at the 0.05 confidence level.

To improve the reliability of our calculations, we also included five samples of <180 μm sediment collected by the AIST geochemical mapping project (Imai et al., 2004). We combined results from our 180–125, 125–75, and <75 μm fractions in proportion to their weights for compatibility with the AIST samples.

The results of multiple regression analysis are summarized in

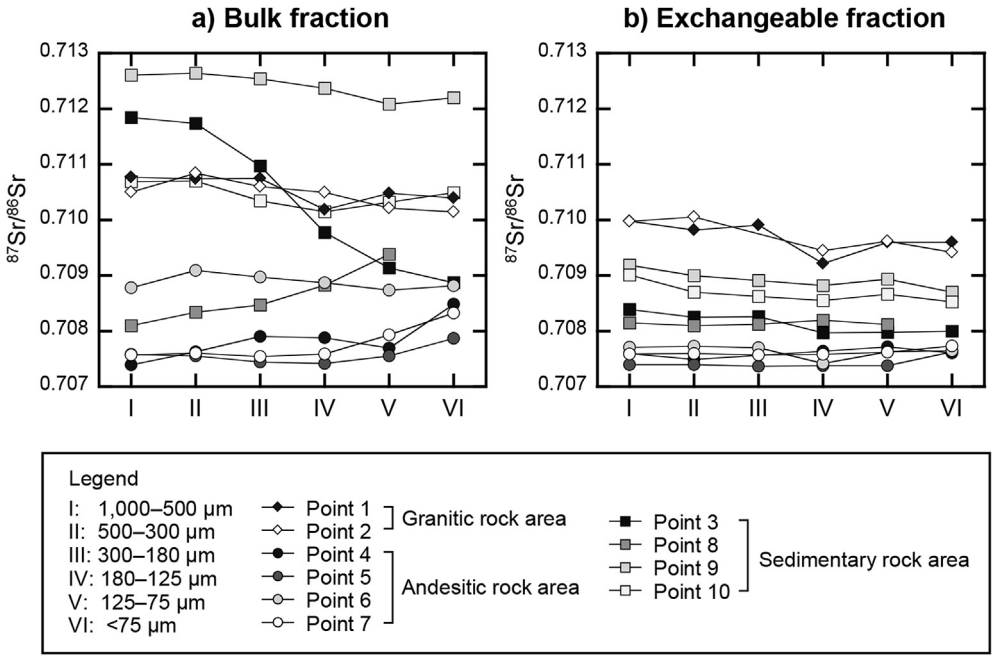

Fig. 3. $^{87}Sr/^{86}Sr$ ratios of the bulk fraction (a) and the Ex fraction (b) of stream sediment samples at different particle sizes.

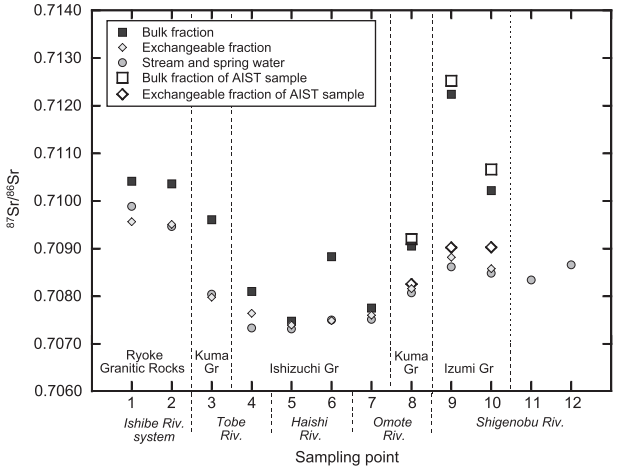

Fig. 4. $^{87}Sr/^{86}Sr$ values of stream sediments and stream water at sampling locations. Values for the bulk and Ex fractions are mean values calculated for the three finest fractions (180–125, 125–75, and <75 μm).

Table 7. The relative standard errors estimated by this analysis were 7–19% for Rb concentration data, 11–27% for Sr concentration data, and 4.5–12.4 ppm for $^{87}Sr/^{86}Sr$. The estimated Rb concentrations and $^{87}Sr/^{86}Sr$ were comparable to their measured values (Fig. 5). The estimated Sr concentrations differed from the original data for Points 3, 4, 6, and 8, which represent watershed areas underlain by rocks of the Kuma Group (Fig. 5).

Fig. 6 shows the relationship between Rb/Sr and $^{87}Sr/^{86}Sr$ for stream sediments and their corresponding source rocks. The estimated Rb/Sr and $^{87}Sr/^{86}Sr$ values for sediments derived from Ryoke granite ($Gr + Rg_{reg}$, where "reg" refers to the estimate based on the regression analysis) were 0.82 ± 0.13 and 0.71039 ± 0.00033 (mean±1σ). Kagami et al. (1988) reported that $^{87}Sr/^{86}Sr$ of Ryoke granitic rocks from Shikoku Island ranged from 0.70813 to 0.71735, and that three granitic rock samples from the Matsuyama area had Rb/Sr ratios of 0.49–0.95 and $^{87}Sr/^{86}Sr$ of 0.70955–0.71113. These values are consistent with those of $Gr + Rg_{reg}$.

The estimated $^{87}Sr/^{86}Sr$ values for andesite (An_{reg}) and Sambagawa greenschist (Sg_{reg}) were 0.70664 ± 0.00049 and 0.70531 ± 0.00050, respectively. The mean estimated Rb/Sr for the combined group ($An + Sg_{reg}$) was 0.19 ± 0.04. Our estimated values for An_{reg} were comparable to those of two andesitic rocks from the Ishizuchi Group (Rb/Sr, 0.16 and 0.27; $^{87}Sr/^{86}Sr$, 0.70600 and 0.70614) reported by Tazaki et al. (1993). Our estimated values for Sg_{reg} were higher than those of Sambagawa greenschist (Rb/Sr, 0.052 ± 0.025; $^{87}Sr/^{86}Sr$, 0.70385 ± 0.00059) reported by Utsunomiya et al. (2011). We attribute this difference to a greater contribution in the study area of pelitic schist with high Rb/Sr (0.60 and 2.63) and $^{87}Sr/^{86}Sr$ (0.710120 and 0.716063) values (Utsunomiya et al., 2011) that is associated with greenschist.

The estimated mean Rb/Sr of the combined sedimentary rock group (Sed_{reg}) was 1.67 ± 0.44, the highest value among our three lithologic groups. The estimated $^{87}Sr/^{86}Sr$ of the Izumi Group (Iz_{reg}) was the highest of all our original lithologic units at 0.71315 ± 0.00054. Rock samples from the Izumi Group also had high values of Rb/Sr and $^{87}Sr/^{86}Sr$ (Table 4), possibly reflecting the presence of K-feldspar in sandstone and acidic volcanic rocks in this unit (Doi, 1964; Miyata et al., 1993). Sandstone sample no. 1 (Table 4) had Rb/Sr of 1.60 and $^{87}Sr/^{86}Sr$ of 0.713498, values consistent with those of Iz_{reg}. The estimated $^{87}Sr/^{86}Sr$ values for the Kuma Group and Quaternary sediments (Ku_{reg} and Qs_{reg}) were comparable to those of the combined Ryoke group ($Gr + Rg_{reg}$, Table 7). It is a reasonable inference that clastics of the Kuma Group originated from Ryoke granite and the Izumi Group (Katto and Taira, 1979). In addition, the Quaternary sediments in the Dougo Plain may have been largely supplied by the Ishide River (Fig. 1), which drains an area underlain by Ryoke granite and Ryoke metamorphic rocks (Suyari et al., 1991). The relatively high Rb/Sr of Sed_{reg} may reflect the predominance of weathering-resistant K-feldspar over plagioclase (Takagi et al., 2001).

5.4. Comparison of $^{87}Sr/^{86}Sr$ in stream water and stream sediment

Systematic lower $^{87}Sr/^{86}Sr$ in stream water and the Ex fraction of stream sediment than in bulk sediment (Fig. 4) may be partly

Table 6
Results of two-way ANOVA applied to elemental concentrations and $^{87}Sr/^{86}Sr$ ratio of stream sediments.

	n	*p* of S-W test[a]		Skewness		Data format for ANOVA	*F* value of two-way ANOVA			*p* of two-way ANOVA[b]			Major factor
		Raw	Log	Raw	Log		Geology[c]	Grain size[c]	Int.[c]	Geology[c]	Grain size[c]	Int.[c]	
SiO_2	54	**0.09**	**0.02**	−0.38	−0.60	Unchanged	13	6.5	0.41	**6×10^{-5}**	**2×10^{-4}**	0.93	Grain size
TiO_2	54	<0.01	<0.01	2.05	0.43	Log-transformed	13	2.4	0.14	<**0.01**	0.06	1.00	Geology
Al_2O_3	54	<0.01	<0.01	0.29	0.14	Log-transformed	5.5	0.83	0.54	<**0.01**	0.54	0.85	Geology
Fe_2O_3	54	**0.04**	**0.12**	0.56	−0.23	Log-transformed	7.2	3.0	0.59	<**0.01**	0.02	0.81	Geology
MnO	54	<0.01	**0.07**	3.00	0.50	Log-transformed	2.3	3.8	0.77	0.11	<**0.01**	0.66	Grain size
MgO	54	**0.03**	**0.02**	0.47	−0.42	Unchanged	29	1.3	0.44	<**0.01**	0.29	0.92	Geology
CaO	54	**0.05**	<0.01	0.21	−0.69	Unchanged	27	0.29	0.39	<**0.01**	0.91	0.94	Geology
Na_2O	54	**0.19**	<0.01	0.07	−0.98	Unchanged	5.7	0.85	0.19	<**0.01**	0.52	1.00	Geology
K_2O	54	**0.11**	**0.36**	0.36	−0.06	Unchanged	42	2.6	0.43	<**0.01**	0.04	0.92	Geology
P_2O_5	54	<0.01	**0.03**	2.59	0.77	Log-transformed	12	3.7	1.1	<**0.001**	**0.008**	0.37	Geology
Ba	52	<0.01	<0.01	0.17	−0.08	Log-transformed	11	0.45	0.18	<**0.01**	0.81	1.00	Geology
Co	52	<0.01	**0.05**	1.32	−0.34	Log-transformed	7.2	2.2	0.40	<**0.01**	0.08	0.94	Geology
Cr	52	**0.05**	<0.01	0.32	−0.80	Unchanged	36	6.2	0.60	**5×10^{-9}**	**3×10^{-4}**	0.80	Geology
Ni	52	<0.01	**0.01**	2.27	0.27	Log-transformed	11	0.53	0.17	<**0.01**	0.75	1.00	Geology
Pb	52	<0.01	<0.01	2.49	1.26	Log-transformed	2.5	1.9	0.15	0.09	0.13	1.00	None
Rb	52	**0.20**	**0.15**	0.11	−0.29	Unchanged	73	2.2	0.43	<**0.01**	0.08	0.92	Geology
Sr	52	<0.01	**0.01**	0.21	−0.18	Log-transformed	9.0	0.28	0.15	<**0.01**	0.92	1.00	Geology
Th	52	<0.01	<0.01	2.78	−1.39	Log-transformed	18	0.07	1.6	<**0.01**	1.00	0.14	Geology
V	52	<0.01	**0.85**	1.27	−0.06	Log-transformed	48	4.6	0.93	<**0.001**	**0.003**	0.52	Geology
Y	52	<0.01	<0.01	2.86	1.86	Log-transformed	47	12	5.6	**2×10^{-10}**	**1×10^{-6}**	**6×10^{-5}**	Geology
Zn	52	<0.01	<0.01	4.22	1.76	Log-transformed	1.4	0.75	0.08	0.26	0.59	1.00	None
Zr	52	<0.01	<0.01	4.15	1.73	Log-transformed	8.6	9.0	2.9	**9×10^{-4}**	**2×10^{-5}**	**0.01**	Grain size
$^{87}Sr/^{86}Sr$	59	<0.01	<0.01	0.34	0.33	Unchanged	34	0.15	0.11	<**0.01**	0.98	1.00	Geology

Raw, raw data; Log, log-transformed data; S-W test, Shapiro-Wilk test; Int., interaction effects.
[a] Boldface type means that the null hypothesis is accepted at $p = 0.01$.
[b] Boldface type means that the null hypothesis is rejected at $p = 0.01$.
[c] Degrees of freedom of geology, grain size, and interaction effects are 2, 5, and 10, respectively.

Table 7
Multiple regression analysis of $^{87}Sr/^{86}Sr$ for 15 stream sediment samples <180 μm.

Representative lithology	$^{87}Sr/^{86}Sr$	Standard deviation	*p* value	Lower 95%	Upper 95%	Variance inflation factor
Gr and Rg	0.71039	0.00033	<0.01	0.70964	0.71113	1.15
Qs	0.71058	0.00090	<0.01	0.70855	0.71261	1.58
Iz	0.71315	0.00054	<0.01	0.71192	0.71438	1.74
Ku	0.71070	0.00062	<0.01	0.70929	0.71210	2.55
An	0.70664	0.00049	<0.01	0.70553	0.70774	2.52
Sg	0.70531	0.00050	<0.01	0.70418	0.70643	1.01

Representative lithology	Rb	Standard deviation	*p* value	Lower 95%	Upper 95%	Variance inflation factor
Gr and Rg	120	8	<0.01	103	136	1.04
Sed (Qs, Iz, and Ku)	127	7	<0.01	112	142	1.33
An and Sg	39	8	<0.01	22	57	1.29

Representative lithology	Sr	Standard deviation	*p* value	Lower 95%	Upper 95%	Variance inflation factor
Gr and Rg	146	21	<0.01	101	192	1.04
Sed (Qs, Iz, and Ku)	76	19	<0.01	34	118	1.33
An and Sg	210	23	<0.01	161	258	1.29

caused by the input of atmospheric aerosols to the surficial sediments and waters. However, the contribution of Asian dust from China and sea-salt aerosols to stream sediment and stream water could be very small because their $^{87}Sr/^{86}Sr$ values are 0.709–0.718 and much higher than those of our samples (Jahn et al., 2001; Kanayama et al., 2002), and because Nakano et al. (2012) reported that only 28% of the Sr^{2+} in stream waters is derived from sea-salt aerosols even in the isolated island of Yakushima, which is located 70 km south of the Japanese mainland and surrounded by a vast sea.

During chemical weathering of granitic rocks, Sr is released from K-feldspar and biotite into groundwater and surface water (Blum et al., 1993; Bullen et al., 1997), resulting in that $^{87}Sr/^{86}Sr$ in groundwater samples is systematically lower than in the host granitic rocks (Takagi et al., 2001). This fact is consistent with our results (Fig. 4). Takagi et al. (2001) suggested that plagioclase, which has a lower $^{87}Sr/^{86}Sr$ than whole rock, is more readily weathered than K-feldspar, biotite, and clay minerals, in which $^{87}Sr/^{86}Sr$ is relatively high. This would explain why $^{87}Sr/^{86}Sr$ is systematically lower in stream water and the Ex fractions of stream sediments than in bulk sediments, similar with the result by Minami and Suzuki (submitted). Andesitic volcanic rocks contain little K-feldspar, biotite, and clay minerals, thus plagioclase would control $^{87}Sr/^{86}Sr$ of whole rock in areas of andesitic volcanic rocks such as Points 5 and 7. Consequently, $^{87}Sr/^{86}Sr$ differs little at Points 5 and 7 among the bulk fraction, Ex fraction, and stream water. In contrast, $^{87}Sr/^{86}Sr$ in stream water and the Ex fraction of sediment at Point 9 and sample 15023, representing the Izumi Group, is much lower than in the corresponding bulk sediment (Table 1 and Fig. 4). As noted above, K-feldspar from sandstone and acidic volcanic

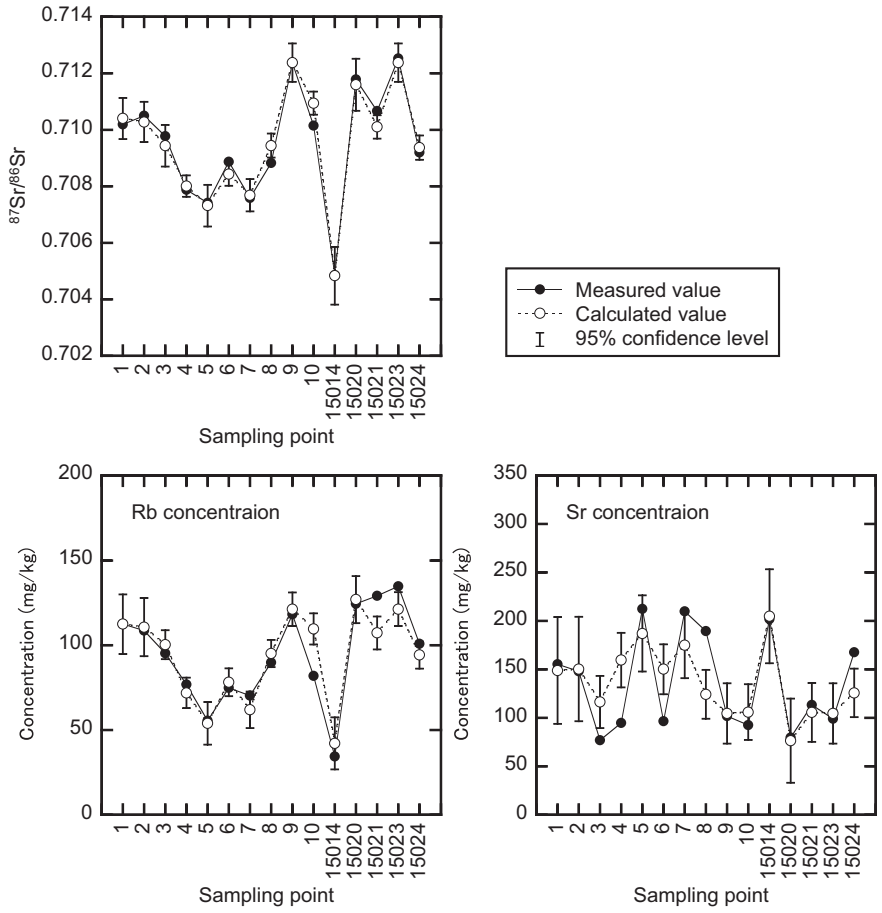

Fig. 5. Multiple regression analysis results for Rb and Sr concentrations and $^{87}Sr/^{86}Sr$ in the combined fine fraction (180–125, 125–75, and <75 μm) of bulk stream sediments.

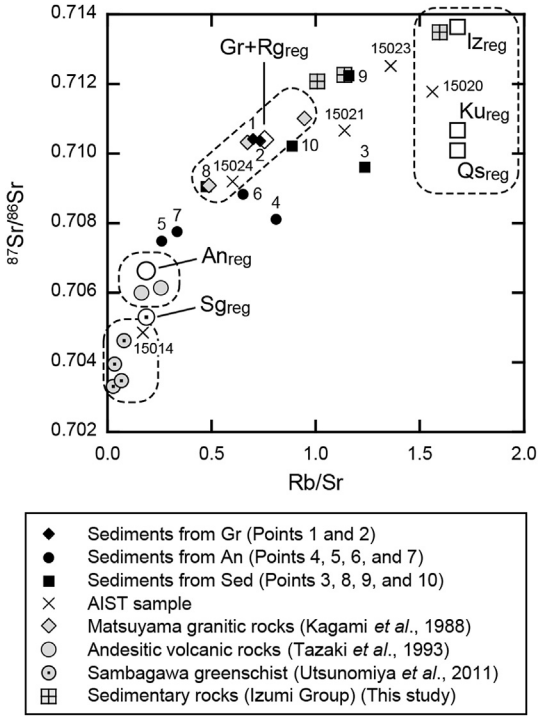

rocks of the Izumi Group was responsible for raising $^{87}Sr/^{86}Sr$ and Rb/Sr in the bulk fraction of these samples (Fig. 6) whereas Ex fraction may selectively extract Sr from plagioclase having lower $^{87}Sr/^{86}Sr$.

The $^{87}Sr/^{86}Sr$ values of bulk sediment were poorly correlated with those of the Ex fraction of stream sediment or stream water on the whole (Fig. 7a). This result means that unlike bulk stream sediment, neither the Ex fraction of stream sediment nor stream water directly reflect $^{87}Sr/^{86}Sr$ in the watershed bedrock. However, $^{87}Sr/^{86}Sr$ values of the Ex fraction of stream sediment were strongly correlated (correlation coefficient = 0.99) with those of stream water samples (Fig. 7b). The Ex fraction of stream sediment would be less sensitive to the episodic events such as flood and drought than stream water samples. Simply, we can assume that the Rb/Sr and $^{87}Sr/^{86}Sr$ values of Ex fractions of stream sediments represent the long-time average of stream waters. Therefore, these results indicate that $^{87}Sr/^{86}Sr$ of the Ex fraction of stream sediment can be used as an approximation of river water.

Fig. 6. Relationship between Rb/Sr and $^{87}Sr/^{86}Sr$ ratios in the fine fraction of bulk stream sediments (180–125, 125–75, and <75 μm) and three groups of host rocks (see Table 7 for definitions). The abbreviation Gr, Rg, An, Sed, Iz, Ku, and Qs indicate the sediments derived from Ryoke granite, Ryoke gneiss, andesitic volcanic rocks, sedimentary rocks, Izumi Group, Kuma Group, and Quaternary sediments, respectively. The "reg" indicated by a subscript refers to the estimate based on the regression analysis.

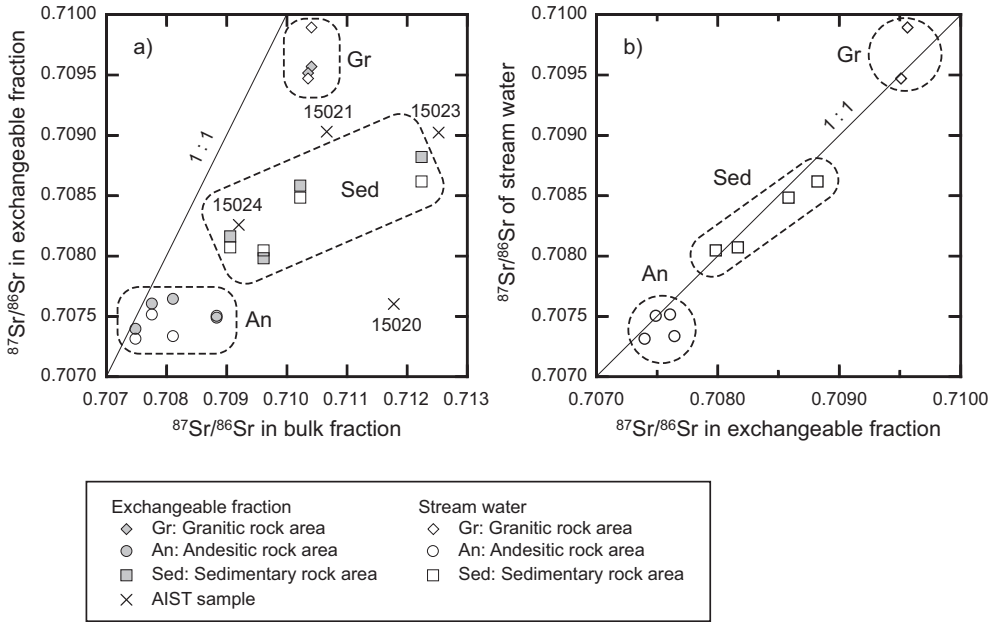

Fig. 7. a) Relationship of $^{87}Sr/^{86}Sr$ in the Ex fraction of stream sediments and the bulk fraction of sediments. b) Relationship of $^{87}Sr/^{86}Sr$ in the Exfraction of stream sediments and stream water. The values for bulk and Ex fraction of stream sediments are mean values for the combined fine fractions (180–125, 125–75, and <75 μm).

6. Summary

This study investigated some problems in creating a regional distribution map of $^{87}Sr/^{86}Sr$ on the basis of stream sediments for provenance study, and we have elucidated some problems: the effects of particle size on elemental concentrations and $^{87}Sr/^{86}Sr$, the most suitable particle size for creating $^{87}Sr/^{86}Sr$ maps that reliably represents the geology of the watershed, and the relationships of $^{87}Sr/^{86}Sr$ in host rocks with $^{87}Sr/^{86}Sr$ in stream water and stream sediment samples. We analyzed elemental concentrations and $^{87}Sr/^{86}Sr$ of stream sediment and stream water samples from the Shigenobu River system, which drains catchments of a variety of rock types. Our findings are as follows.

(1) The concentration of most elements increased in the smaller stream sediment fractions regardless of rock type. In particular, P_2O_5 and Zr concentrations were especially high in the finest fraction (<75 μm) of samples from granitic areas, and the highest concentrations of TiO_2, Fe_2O_3, MgO, and V in samples from andesitic areas were in the medium fraction (300–75 μm). On the other hand, concentrations of SiO_2, Na_2O, K_2O, Rb, and Ba decreased with decreasing particle size. Concentrations of Sr varied little with particle size. We attribute these variations mainly to differences in the mineral composition of the host rocks, differences in resistance to weathering of major minerals, and differences in the resulting abundances of specific minerals in specific particle-size fractions.

(2) The variation with particle size in $^{87}Sr/^{86}Sr$ of stream sediment (within approximately 0.001) was smaller than the variation across the bedrock units of the watersheds. The $^{87}Sr/^{86}Sr$ of sediments corresponded well to $^{87}Sr/^{86}Sr$ in the aggregate blend of their host rocks, as estimated using multiple regression analysis. Stream water samples had systematically lower $^{87}Sr/^{86}Sr$, with smaller variations, than the stream sediment at the same sites. However, the $^{87}Sr/^{86}Sr$ of stream water corresponded closely to $^{87}Sr/^{86}Sr$ of the Ex fraction of stream sediment at the same sites, and both systematically reflected the lithology of their watershed areas, being low in areas of andesitic volcanic rocks and high in areas of granitic rocks.

These findings suggest that stream sediment reflects the elemental concentrations and $^{87}Sr/^{86}Sr$ of its watershed regardless of particle size. We also found that stream water and the Ex fraction of stream sediment yield essentially the same $^{87}Sr/^{86}Sr$. Finally, we conclude that the <180 μm fraction of stream sediment, which has been widely collected for geochemical mapping purposes, can also be reliably utilized in creating a nationwide $^{87}Sr/^{86}Sr$ map.

Acknowledgments

Measurement of $^{87}Sr/^{86}Sr$ was performed using a thermal ionization mass spectrometer with the assistance of Dr. Yoshihiro Asahara of Nagoya University. We were assisted with X-ray fluorescence spectrometry by Dr. Takenori Kato of Nagoya University. Rock samples (one conglomerate and two sandstones) from the Izumi Group were supplied by Dr. Atsushi Noda of AIST. This study was supported by KAKENHI Grant Number 22300308 from the Ministry of Education, Culture, Sports, Science and Technology. The anonymous reviewers are acknowledged for their constructive comments of the manuscript.

References

Aoya, M., Noda, A., Mizuno, K., Mizukami, T., Miyachi, Y., Matsuura, H., Endo, S., Toshimitsu, S., Aoki, M., 2013. Geology of the Niihama district. Quadrangle series, 1:50,000 13 Kochi-40. Geol. Surv. Jpn. AIST (in Japanese, with English abstract).

Asahara, Y., Ishiguro, H., Tanaka, T., Yamamoto, K., Mimura, K., Minami, M., Yoshida, H., 2006. Application of Sr isotopes to geochemical mapping and provenance analysis: the case of Aichi Prefecture, central Japan. Appl. Geochem 21, 419–436.

Bataille, C.P., Bowen, G.J., 2012. Mapping $^{87}Sr/^{86}Sr$ variations in bedrock and water for large scale provenance studies. Chem. Geol. 304–305, 39–52.

Bataille, C.P., Brennan, S.R., Hartmann, J., Moosdorf, N., Wooller, M.J., Bowen, G.J., 2014. A geostatistical framework for predicting variations in strontium concentrations and isotope ratios in Alaskan rivers. Chem. Geol. 389, 1–15.

Bentley, R.A., 2006. Strontium isotopes from the earth to the archaeological skeleton: a review. J. Archaeol. Method Theory 13, 135–187.

Blum, J.D., Erel, Y., Brown, K., 1993. $^{87}Sr/^{86}Sr$ ratios of Sierra-Nevada stream waters: implications for relative mineral weathering rates. Geochim. Cosmochim. Acta 57, 5019–5025.

Bouchez, J., Metivier, F., Lupker, M., Maurice, L., Perez, M.A., Gaillardet, J., France-Lanord, C., 2010. Prediction of depth-integrated fluxes of suspended sediment in the Amazon River: particle aggregation as a complicating factor. Hydrol. Process. 25, 778–794.

Bouchez, J., Gaillardet, J., France-Lanord, C., Maurice, L., Dutra-Maia, P., 2011. Grain size control of river suspended sediment geochemistry: clues from Amazon River depth profiles. Geochem. Geophys. Geosyst. 12, Q03008.

Brennan, S.R., Torgersen, C.E., Hollenbeck, J.P., Fernandez, D.P., Jensen, C.K., Schindler, D.E., 2016. Dendritic network models: improving isoscapes and quantifying influence of landscape and in-stream processes on strontium isotopes in rivers. Geophys. Res. Lett. 43, 5043–5051. https://doi.org/10.1002/2016GL068904.

Caritat, P. de, Cooper, M., 2011. National geochemical Survey of Australia: data quality assessment. Geoscience. Australia Record 2011/21. http://www.ga.gov.au/corporate_data/71971/Rec2011_021_Vol1.pdf.

Chiba, E., Sakakibara, M., Sano, S., Hori, R.S., Nakai, Y., 2005. Behavior of major and trace elements of the Mannen altered andesite during chemical weathering in the Tobe Town, Ehime Prefecture, Japan. Men. Fac. Sci. Ehime Univ. 11, 39–46 (in Japanese, with English abstract).

Crowley, B.E., Miller, J.H., Bataille, C.P., 2015. Strontium isotopes ($^{87}Sr/^{86}Sr$) in terrestrial ecological and palaeoecological research: empirical efforts and recent advances in continental-scale models. Biol. Rev. 92, 43–59.

Doi, M., 1964. Mishima. Geological map of Japan 1:50,000. Geol. Surv. Jpn.

Fauth, H., Hindel, R., Siewers, U., Zinner, J., 1985. Geochemischer Atlas Bundesrepublik Deutschland. Bundesanstatt für Geowissenschaften and Rohstoffe (BGR), Hannover.

Frei, K.M., Frei, R., Mannering, U., Gleba, M., Nosch, M.L., Lyngstrøm, H., 2009. Provenance of ancient textiles -A pilot study evaluating the strontium isotope system in wool. Archaeometry 51, 252–276.

Goldich, S.S., 1938. A study in rock-weathering. Jour. Geol. 46, 17–58.

Graustein, W.C., 1989. $^{87}Sr/^{86}Sr$ ratios measure the sources and flow of strontium in terrestrial ecosystems. Stable isotopes in ecological research. Ecol. Stud. 68, 491–512.

Hodell, D.A., Quinn, R.L., Brenner, M., Kamenov, G., 2004. Spatial variation of strontium isotopes ($^{87}Sr/^{86}Sr$) in the Maya region: a tool for tracking ancient human migration. J. Archaeol. Sci. 31, 585–601.

Howarth, R.J., Thornton, I., 1983. Regional geochemical mapping and its application to environmental studies. In: Thornton, I. (Ed.), Applied Environmental Geochemistry. Academic Press, London, pp. 41–73.

Imai, N., Terashima, S., Ohta, A., Mikoshiba, M., Okai, T., Tachibana, Y., Togashi, S., Matsuhisa, Y., Kanai, Y., Kamioka, H., Taniguchi, M., 2004. Geochemical map of Japan. Geol. Surv. Jpn. AIST, Tsukuba. Available at: https://gbank.gsj.jp/geochemmap/.

Jahn, B.M., Gallet, S., Han, J.M., 2001. Geochemistry of the Xining, Xifeng and Jixian sections, Loess Plateau of China: eolian dust provenance and paleosol evolution during the last 140 ka. Chem. Geol. 178, 71–94.

Japan Meteorological Agency. Past precipitation data in Matsuyama. Available at: http://www.data.jma.go.jp/gmd/risk/obsdl/.

Jomori, Y., Minami, M., Ohta, A., Takeuchi, M., Imai, N., 2013. Spatial distribution of $^{87}Sr/^{86}Sr$ ratios of stream sediments in Shikoku island and the Kii Peninsula, southwest Japan. Geochem. J. 47, 321–335.

Kagami, H., Honma, H., Shirahase, T., Nureki, T., 1988. Rb-Sr whole rock isochron ages of granites from northern Shikoku and Okayama, southwest Japan: implications for the migration of the Late Cretaceous to Paleogene igneous activity in space and time. Geochem. J. 22, 69–79.

Kanayama, S., Yabuki, S., Yanagisawa, F., Motoyama, R., 2002. The chemical and strontium isotope composition of atmospheric aerosols over Japan: the contribution of long-range-transported Asian dust (Kosa). Atmos. Environ. 36, 5159–5175.

Katto, J., Taira, A., 1979. New observation of the Kuma group. Chishitsu News 293, 12–21 (in Japanese).

Kawasaki, A., Oda, H., Hirata, T., 2002. Determination of strontium isotope ratio of brown rice for estimating its provenance. Soil Sci. Plant Nutr. 48, 635–640.

Kihara, S., 1985. Stratigraphy and paleoenvironment of the Kuma group around the Kuma town in central Ehime prefecture, Shikoku. In: Memoirs of the Symposium on Formation of Slump Facies and its Relation to Tectonics –Some Problems on the Deformation of Unconsolidated Sediments, pp. 133–144 (in Japanese, with English abstract).

Miller, J.C., Miller, J.N., 2010. Statistics for Analytical Chemistry, sixth ed. Pearson Education Canada.

Minami, M., Jomori, Y., Suzuki, K., Ohta, A., 2017. Grain-size variations in $^{87}Sr/^{86}Sr$ and elemental concentrations of stream sediments in a granitic area: fundamental study on $^{87}Sr/^{86}Sr$ spatial distribution mapping. Geochem. J. https://doi.org/10.2343/geochemj.2.0478.

Minami, M., Suzuki, K. Relationship between $^{87}Sr/^{86}Sr$ in geological samples and biological samples: case study of rice plants in granitic bedrock area in Japan. (submitted to Chemical Geology).

Miyaji, K., Tsuzuki, Y., 1988. Hydrothermal alteration genetically related to the mannen and uebi pottery stone deposits in tobe district, Ehime prefecture. J. Clay Sci. Soc. Jpn. 28, 183–199 (in Japanese, with English abstract).

Miyata, T., Makimoto, H., Sangawa, A., Ichikawa, K., 1993. Geology of the wakayama and ozaki distrivt, with geological sheet map at 1:50,000. Geol. Surv. Jpn.

Miyazaki, K., Wakita, K., Miyashita, Y., Mizuno, K., Takahashi, M., Noda, A., Toshimitsu, S., Sumii, T., Ohno, T., Nawa, K., Miaykawa, A., 2016. Geological map of Japan 1:200,000, Matsuyama (2nd edition). Geol. Surv. Jpn.

Nagai, K., 1957. The upper Eocene flora of the Kuma group, in the Ishizuchi range, Shikoku, Japan. Mem. Ehime Univ. Sect-II 2, 73–82.

Nakano, T., Yokoo, Y., Okumura, M., Jean, S.R., Satake, K., 2012. Evaluation of the impacts of marine salts and Asian dust on the forested Yakushima island ecosystem, a world natural heritage site in Japan. Water Air Soil Pollut. 223, 5575–5597.

Ohta, A., Imai, N., Terashima, S., Tachibana, Y., Ikehara, K., Nakajima, T., 2004. Geochemical mapping in Hokuriku, Japan: influence of surface geology, mineral occurrences and mass movement from terrestrial to marine environments. Appl. Geochem 19, 1453–1469.

Ohta, A., Imai, N., Terashima, S., Tachibana, Y., 2005. Application of multi-element statistical analysis for regional geochemical mapping in Central Japan. Appl. Geochem 20, 1017–1037.

Ohta, A., Imai, N., Terashima, S., Tachibana, Y., Ikehara, K., Katayama, H., Noda, A., 2010. Factors controlling regional spatial distribution of 53 elements in coastal sea sediments in northern Japan: comparison of geochemical data derived from stream and marine sediments. Appl. Geochem 25, 357–376.

Reimann, C., Äyräs, M., Chekushin, V., Bogatyrev, I., Boyd, R., Caritat, P. d., Dutter, R., Finne, T.E., Halleraker, J.H., Jæger, Ø., Kashulina, G., Lehto, O., Niskavaara, H., Pavlov, V., Räisänen, M.L., Strand, T., Volden, T., 1998. Environmental geochemical atlas of the central barents region. Geol. Surv. Nor. Trondheim, Nor.

Rummel, S., Hoelzl, S., Horn, P., Rossmann, A., Schlicht, C., 2010. The combination of stable isotope abundance ratios of H, C, N and S with $^{87}Sr/^{86}Sr$ for geographical origin assignment of orange juices. Food Chem. 118, 890–900.

Sakakibara, M., Nakai, Y., Chiba, E., Chikaishi, S., Sano, S., Hori, R.S., 2005. Mode of occurrence of sulfide minerals and arsenic concentration of boring core samples in Mannen altered andesite of the Tobe Town, Ehime Prefecture, Japan. Men. Fac. Sci. Ehime Univ. 11, 27–37 (in Japanese, with English abstract).

Salminen, R., Batista, M.J., Bidovec, M., Demetriades, A., De Vivo, B., De Vos, W., Duris, M., Gilucis, A., Gregorauskiene, V., Halamic, J., Heitzmann, P., Lima, A., Jordan, G., Klaver, G., Klein, P., Lis, J., Locutura, J., Marsina, K., Mazreku, A., O'Connor, P.J., Olsson, S.Å., Ottesen, R.-T., Petersell, V., Plant, J.A., Reeder, S., Salpeteur, I., Sandström, H., Siewers, U., Steenfelt, A., Tarvainen, T., 2005. Geochemical atlas of europe. Part 1-background information, methodology and maps. Geol. Surv. Finl. Espoo, Finl.

Shapiro, S.S., Wilk, M.B., 1965. An analysis of variance test for normality (complete samples). Biometrika 52, 591–611.

Smith, D.B., Cannon, W.F., Woodruff, L.G., Solano, F., Ellefsen, K.J., 2014. Geochemical and Mineralogical Maps for Soils of the Conterminous United States. U.S. Geological Survey Open-File Report 2014-1082. http://pubs.usgs.gov/of/2014/1082/pdf/ofr2014-1082.pdf.

Suyari, K., Iwasaki, M., Suzuki, T., 1991. Regional Geology of Japan Part 8 (SHIKOKU). Kyoritsu Shuppan Co, 284 pp (in Japanese).

Takagi, M., Tanaka, T., Asahara, Y., Aoki, K., Amano, K., 2001. Chemical weathering of rocks in the view of Sr isotopic ratio: study of groundwater at Kamaishi mine. Chikyukagaku Geochem. 35, 61–72 (in Japanese, with English abstract).

Tazaki, K., Kagami, H., Itaya, T., Nagao, T., 1993. K-Ar ages and the origin of acidic volvanit rocks along the Median Tectonic Line at northwest Shikoku. Jpn. Mem. Geol. Soc. Jpn. 42, 267–278 (in Japanese, with English abstract).

Terashima, S., Imai, N., Ikehara, K., Katayama, H., Okai, T., (Ujiie) Mikoshiba, M., Ohta, A., Kubota, R., 2008. Variation of elemental concentrations of river and marine sediments according to the grain size classification. Bull. Geol. Surv. Jpn. 59, 439–459 (in Japanese, with English abstract).

Thornton, E.K., 2011. Reconstructing ancient Maya animal trade through strontium isotope ($^{87}Sr/^{86}Sr$) analysis. J. Archaeol. Sci. 38, 3254–3263.

Utsunomiya, A., Jahn, B.M., Okamoto, K., Ota, T., Shinjoe, H., 2011. Intra-oceanic island arc origin for Iratsu eclogites of the Sanbagawa belt, central Shikoku, southwest Japan. Chem. Geol. 280, 97–114.

Voerkelius, S., Lorenz, G.D., Rummel, S., Quetel, C.R., Heiss, G., Baxter, M., Brach-Papa, C., Deters-Itzelsberger, P., Hoelzl, S., Hoogewerff, J., Ponzevera, E., Van Bocxstaele, M., Ueckermann, H., 2010. Strontium isotopic signatures of natural mineral waters, the reference to a simple geological map and its potential for authentication of food. Food Chem. 118, 933–940.

Weaver, T.A., Broxton, D.E., Bolivar, S.L., Freeman, S.H., 1983. The Geochemical Atlas of Alaska: Compiled by the Geochemistry Group. Earth Sciences Division, Los Alamos National Laboratory, GJBX-32(83), Los Alamos.

Webb, J.S., Thornton, I., Thompson, M., Howarth, R.J., Lowenstein, P.L., 1978. The Wolfson Geochemical Atlas of England and Wales. Clarendon Press, Oxford.

White, A.F., Blum, A.E., Schulz, M.S., Bullen, T.D., Harden, J.W., Peterson, M.L., 1996. Chemical weathering of a soil chronosequence on granitic alluvium: 1. Reaction rates based on changes in soil mineralogy. Geochim. Cosmochim. Acta 60, 2533–2550.

White, A., Blum, A., Harden, J., Schulz, M., 1997. Chemical weathering of a soil chronosequence on granitoid alluvium: 2. Mineralogic and isotopic constraints on the behavior of strontium. Geochim. Cosmochim. Acta 61, 291–306.

Yagishita, K., Nirasawa, M., Saito, K., Terui, K., 2000. Compositional characteristics of Holocene sands in a mature magmatic arc belt : a case study of river sands derived from plutonic and accretionary complexes, northeast Japan. Mem. Geol. Soc. Jpn. 57, 19–28 (in Japanese, with English abstract).

Zheng, C., 1994. Atlas of Soil Environmental Background Value in the People's Republic of China. China Environmental Science Press, Beijing.